

## Catalytic Pyrolysis of Biomass with Fe/La/SBA-15 Catalyst using TGA–FTIR Analysis

Yuli Zhang, Rui Xiao,\* Xiaoli Gu, Huiyan Zhang, Dekui Shen, and Guangying He

Biomass pyrolysis or gasification can convert low-energy density biomass into a high-energy density gaseous fuel. In this paper, pyrolysis of pine sawdust with and without the addition of a catalyst was investigated using a thermogravimetric analyzer coupled with Fourier transform infrared spectroscopy (TGA-FTIR). The effects of modified SBA-15 catalysts on the formation characteristics of CO, CO<sub>2</sub>, and CH<sub>4</sub> were studied. The two prepared catalysts, La/SBA-15 and Fe/La/SBA-15, retained the hexagonal order of the SBA-15 material and showed high thermal stability in the temperature range of the TGA-FTIR experiments. The results showed that the pyrolysis behavior of biomass is remarkably improved in the presence of La/SBA-15 and Fe/La/SBA-15 catalysts. The modified SBA-15 materials favored thermal cracking of macromolecular substances, resulting in an apparent decrease in the tar and coke fraction, an increase in the yield of light gases, and much higher gas production. Meanwhile, a significant increase in CH<sub>4</sub> led to a much higher energy density gaseous product.

*Keywords:* Biomass; Catalytic pyrolysis; TGA-FTIR; SBA-15

*Contact information:* Key Laboratory of Energy Thermal Conversion and Control of Ministry of Education, Southeast University, Nanjing 210096, PR China; \*Corresponding author: ruixiao@seu.edu.cn

### INTRODUCTION

Biomass is an attractive alternative renewable energy source compared to traditional fossil fuels since it is indigenous, abundant, and environmentally friendly. Utilization of biomass can help to mitigate climate change. Biomass can be converted into valuable chemicals and energy products through various thermo-chemical processes.

Biomass gasification or pyrolysis can convert the low-energy density biomass into a gaseous fuel with much higher heating value. The gasification or pyrolysis of biomass is a complex chemical process that convert biomass into syngas, tar, and char at high temperatures (Scott *et al.* 1985; Raveendran and Ganesh 1996; Chen and Leung 2003; Devi *et al.* 2003; Ren *et al.* 2013). The distribution of the primary products is primarily determined by the operating conditions (*e.g.*, temperature, catalysts, and residue time). For high conversion efficiency, there are a number of reports (Dayton 2002; Devi *et al.* 2003; Abu El-Rub *et al.* 2004) concerning the possible routes to translate the non-degradable tar into valuable gas products. Using tar cracking catalysts is an effective method to achieve that target (Abu El-Rub *et al.* 2004). Some synthesized catalysts, which incorporate active species for tar cracking into a proper catalyst support with appropriate auxiliaries, may help to improve the catalytic performance (Richardson and Gray 1997; Carlson *et al.* 2008; Wang *et al.* 2010; Nguyen *et al.* 2013; Zhang *et al.* 2013a;b). Meanwhile, a much higher energy density gaseous product can be obtained if

the applied catalysts can be used to adjust the gas composition and improve the selectivity of the gases (*e.g.*, CH<sub>4</sub>) with high heating value.

SBA-15 is a neutral, mesoporous material with a large surface area and uniform hexagonal pores. Compared to MCM-41, it shows a higher thermal and hydrothermal stability due to thicker pore walls (Sun *et al.* 2006). Although SBA-15 has little catalytic activity, its mesoporous structure allows for the cracking of large molecules into smaller compounds (Lu *et al.* 2009). Because of these advantages, SBA-15 is considered a promising catalyst support that can lead to better active species dispersion and higher catalytic efficiency. Metallic iron (Tamhankar *et al.* 1985; Nordgreen *et al.* 2006) is catalytically active for reducing the heavy hydrocarbons in the product gas. Work by Martinez *et al.* (2004) showed that the addition of lanthanum to a Ni-Al catalyst resulted in higher carbon conversion into valuable gases and less coke formation over the catalyst. Lansink Rotgerink *et al.* (1988) concluded that the methanation of carbon monoxide over Ni-Al catalysts was enhanced in the presence of La<sub>2</sub>O<sub>3</sub> and that the heating value increased with the methane molar concentration.

In this investigation, a Fe/La/SBA-15 catalyst was synthesized by incorporating iron and lanthanum into the SBA-15 mesoporous material. Pine sawdust was chosen as the biomass material. The catalytic pyrolysis behavior of the biomass in an inert atmosphere was studied in a TGA-FTIR (thermogravimetric analyzer coupled with Fourier transform infrared spectrometer) system with online gas analysis. The weight loss of the biomass sample with temperature was recorded automatically, and the pyrolysis vapors of the pine sawdust were removed from the TGA with the carrier gas and detected by the FTIR on-line. The effects of the catalysts on the composition of the gas evolved during the thermal pyrolysis of pine sawdust were investigated.

## EXPERIMENTAL

### Biomass Feedstock

The biomass feedstock was pine sawdust from Nanjing, Jiangsu province, China. The pine sawdust was ground and then dried at 80 °C for 2 h before the experiment. The proximate and ultimate analyses of the pine sawdust powder are described in Table 1.

**Table 1.** Proximate and Ultimate Analyses of Pine Sawdust Samples

Sample	Pine sawdust	
Proximate analysis (air dried, wt %)	Moisture	9.27
	Volatile	76.64
	Fixed carbon	12.74
	Ash	1.35
Ultimate analysis (air dried, wt %)	C <sub>ad</sub>	44.19
	H <sub>ad</sub>	5.31
	O <sub>ad</sub>	39.78
	N <sub>ad</sub>	0.10
Low heating value (MJ/kg)	LHV	18.91

### Synthesis of the Mesoporous Material

As a support for the active phase, pure silicon SBA-15 was synthesized at Nanjing Forestry University according to the procedure proposed by (Zhao *et al.* 1998). The La/SBA-15 catalyst was synthesized by an *in-situ* hydrothermal method. A mixture of 35

mL of an HCl (2 M) aqueous solution and 15 mL of deionized water was used as the acid source. Two grams of P123 (amphiphilic triblock copolymer poly (ethylene oxide) - poly (propylene oxide) - poly (ethylene oxide); MW = 5800; Aldrich Chemical) was dissolved in this aqueous solution with stirring for about 4 h at 40 °C. Then, 14 mL of TEOS (tetraethyl-orthosilicate) was added and the mixture was stirred for another 1 h. Subsequently, 10 mL of lanthanum nitrate solution (0.1 mol/L) was added to the mixture and the mixture was continuously stirred for 24 h at 40 °C, and the gel mixture was allowed to crystallize in a Teflon-lined autoclave at 100 °C for 24 h. After cooling to room temperature, the solid product was filtered and dried at room temperature. The template agent was removed upon calcination at 550 °C for 6 h, with a heating rate of 1 °C/min, and the La/SBA-15 catalyst prepared.

The Fe/La/SBA-15 was prepared by impregnation. Three grams of Fe (NO<sub>3</sub>)<sub>3</sub> · 9H<sub>2</sub>O was added to 50 mL of ethanol. The prepared La/SBA-15 powder was then immersed into an ethanolic solution of Fe (NO<sub>3</sub>)<sub>3</sub>, with stirring, for about 9 h at 110 °C. After the ethanol was completely evaporated, the sample was calcined atmospherically at 550 °C for 2 h.

### TG-FTIR

A thermogravimetric analyzer (TGA) (TGA92, Setaram) coupled with a Fourier transform infrared (FTIR) spectrometer (Vector22, Bruker) was used to investigate the stability of the catalysts and the pyrolysis of pine sawdust. In the catalytic runs, a mixture of 10 mg of pine sawdust with 50 mg of catalyst was placed into a TGA crucible, while a mixture of 10 mg of pine sawdust with 50 mg of inert quartz sand was used in the non-catalytic control experiments. All the tests were performed under a high-purity nitrogen atmosphere. The primary operating parameters are listed in Table 2. Experiments were carried out from 25 to 1000 °C at a heating rate of 20 °C/min, and samples were held at 1000 °C for another 15 min. Both the pine sawdust and the catalysts were fully dried before the experiments. Pyrolysis vapors released from the pine sawdust were introduced into the FTIR spectrometer through a transfer tube, which was kept at about 200 °C to prevent the condensation of vapor on the tube wall. Evolved gases from the TGA were detected online by the FTIR spectrometer. Based on the integral value of the release curves under specific IR absorptions, the concentration of the gaseous products could be determined. For these experiments, there was about a 100-s delay between obtaining the TGA result and the corresponding IR spectra.

**Table 2.** Experimental Conditions of TG-FTIR

Parameters	Operation Parameters
Samples	Pine sawdust
Biomass particle size	< 0.1mm
Sample mass	10 mg
Catalyst	SBA-15, La/SBA-15, Fe/La/SBA-15
Catalyst particle size	< 0.1 mm
Catalyst mass	50 mg
Carrier gas	99.999% high-purity nitrogen, 65 ml/min
Pressure	1 atm
Temperature	25 to 1000 °C
Heating rate	20 °C/min

## RESULTS AND DISCUSSION

### Catalyst Characterization

The material properties of the ordered mesoporous structure of the modified SBA-15 samples were obtained by XRD and N<sub>2</sub>-adsorption measurements. Figure 1 shows the X-ray diffractographs, corresponding to samples of SBA-15, La/SBA-15, and Fe/La/SBA-15, at low angles. The XRD patterns of the two samples showed three diffraction peaks indexed to [100], [110] and [200], which indicated that the synthetic La/SBA-15 and Fe/La/SBA-15 catalysts maintained the ordered hexagonal mesostructures of the SBA-15 material (Chen *et al.* 2004).

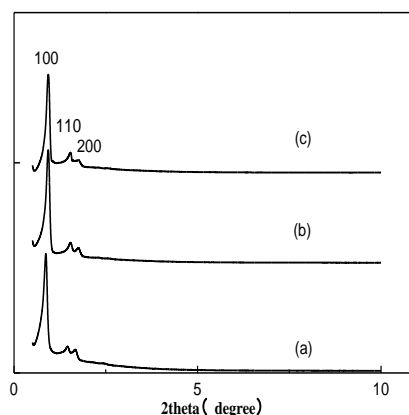


**Fig. 1.** X-ray diffractograms for SBA-15 (a), La/SBA-15 (b), and Fe/La/SBA-15 (c) at low angles

Figure 2 shows the nitrogen adsorption-desorption isotherms and pore size distributions of the different SBA 15 materials. Typical type IV adsorption isotherms (Sing *et al.* 1985), with a H1-type hysteresis loop due to capillary condensation, were observed for all the catalysts. This implied that the modified La/SBA-15 and Fe/La/SBA-15 samples had the characteristic of mesoporous materials. Compared with SBA-15, the capillary condensation step on the nitrogen adsorption isotherm of the modified samples appeared to be narrower. Sharp inflections for P/P<sub>0</sub> values between 0.5 and 0.8 indicated uniform distribution of pore sizes, as showed in Fig. 3. Because of the presence of La and Fe in the silica walls, the average pore size decreased to 6.3 nm (La/SBA-15) and 5.9 nm (Fe/La/SBA-15), as compared to 7.2 nm for SBA-15, which is similar to values found in the literature (Groen *et al.* 2003; Bendahou *et al.* 2008).

### Catalyst Thermostability

To ensure the accuracy of the biomass thermogravimetric experiment results, the stability of the three SBA-15 catalysts was tested in the TGA prior to catalytic biomass pyrolysis. Figure 3 shows the weight loss (TG) and the weight-loss rate (DTG) curves of the three SBA-15 samples. The weight loss of both catalysts mostly occurred below 300 °C. This was because the SBA-15 catalyst support was a mesoporous material with significant moisture content. The moisture was almost completely removed before reaching 300 °C. Almost no weight loss occurred during heating from 300 to 1000 °C, which indicated that the SBA-15, La/SBA-15, and Fe/SBA-15 catalysts all had good thermostability over the temperature range examined. Consequently, the TG-FTIR analysis of catalytic biomass pyrolysis required an intensive drying process.

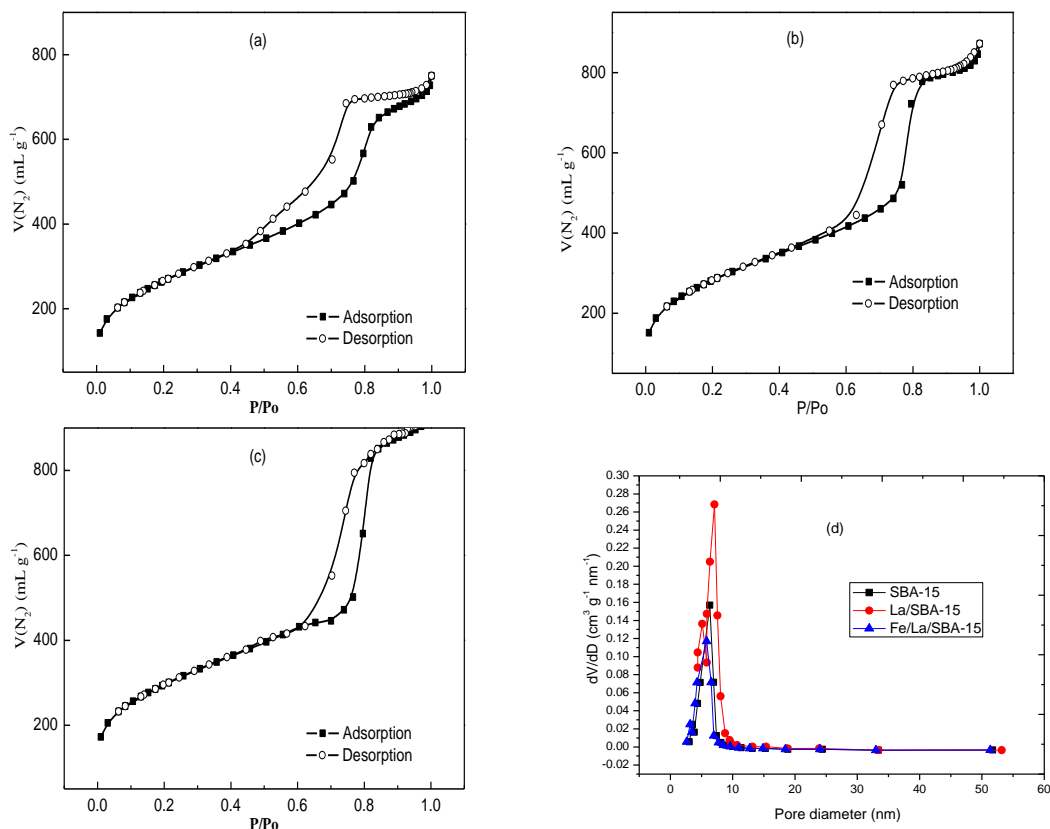


**Fig. 2.** Nitrogen adsorption-desorption isotherms for SBA 15 (a), La/SBA 15 (b), and Fe/La/SBA-15 (c); pore size distributions for SBA 15, La/SBA 15, and Fe/La/SBA-15 (d)

### TG and DTG Analyses

Figure 4 shows the TG and the DTG curves for pine sawdust in catalytic and non-catalytic circumstances. There was one major weight-loss stage in the temperature range of about 300 to 400 °C utilizing a non-catalytic pyrolysis run. Biomass has three main components of hemicellulose, cellulose, and lignin. The cellulose and lignin content in the pine sawdust was as high as 80%, so the pyrolysis of cellulose and lignin played a dominant role.

It has been well established (Nguyen *et al.* 1981; Koufopoulos *et al.* 1989; Yang *et al.* 2007) that hemicellulose decomposition is dominant in the temperature range of about 150 to 350 °C, whereas cellulose mostly decomposes at 350 to 500 °C. Lignin will decompose over a much wider temperature range at temperatures higher than 350 °C because of lignin having larger “thermal resistance” than hemicellulose and cellulose. Therefore, from the different pyrolysis characters of pine sawdust shown in Fig. 4, it can be concluded that, due to the small amount of hemicelluloses in the pine sawdust material, the weight loss below 350 °C during the pine sawdust pyrolysis process was relatively small. Also it is understood that the decomposition of cellulose and lignin mainly contributes to the main weight-loss stage, while lignin mainly contributes to residue char in the higher temperature range.

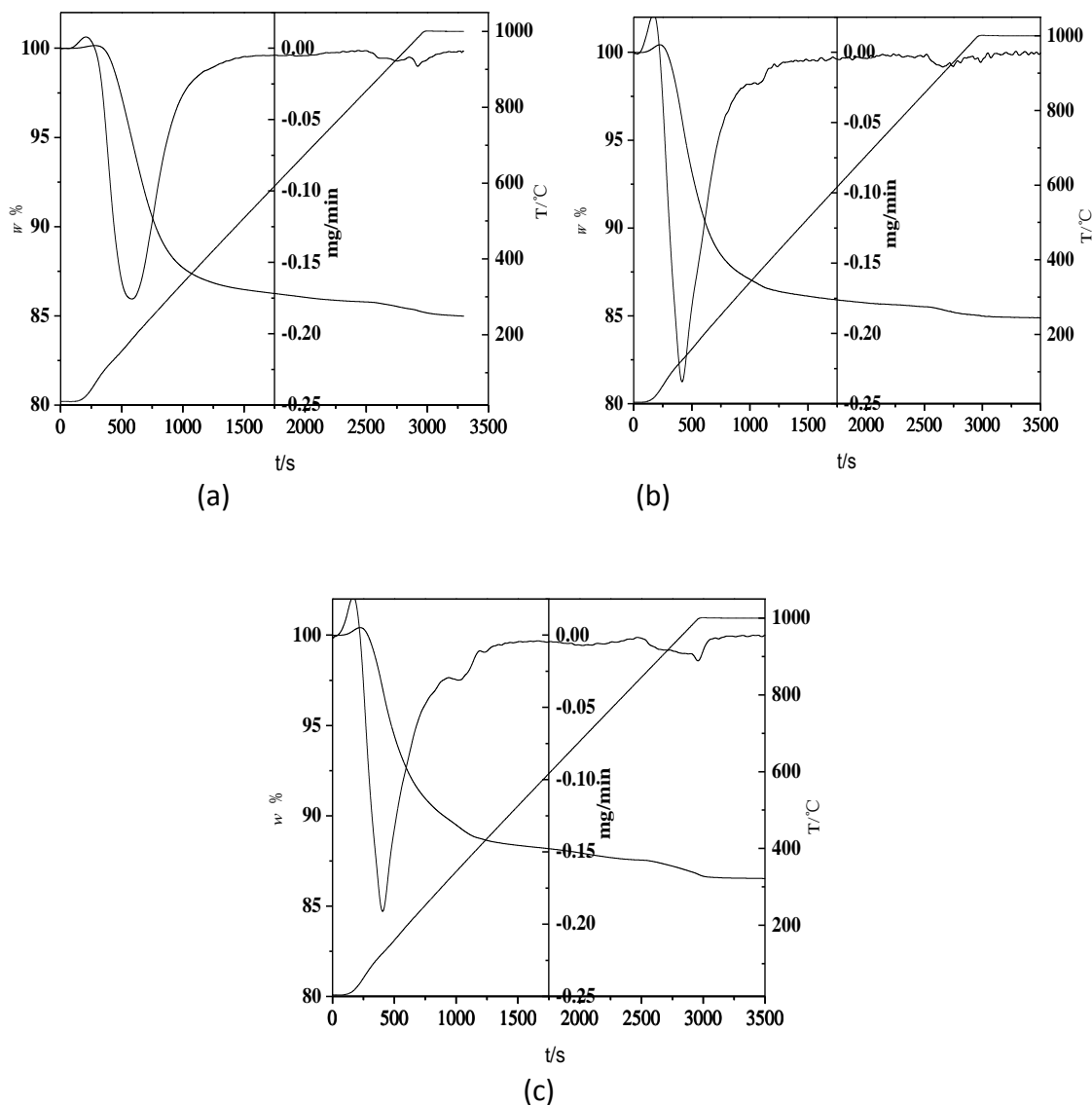


**Fig. 3.** TG and DTG curves of SBA-15 (a), La/SBA-15 (b), and Fe/La/SBA-15 (c)

Table 3 presents the characteristic points of the TG and DTG curves in Fig. 4. The major weight-loss stages all appeared in the temperature range of approximately 300 to 400 °C, with or without catalysts. From a comparison with the non-catalytic control experiments, it can also be observed that the DTG curves from all the runs showed a major weight-loss peak at 373° C (non-catalytic) and 376 °C (SBA-15, La/SBA-15, and Fe/La/SBA-15), respectively. According to Table 3, the presence of catalysts resulted in a decrease in the  $(dw/dt)_{\max}$  and the delay of the start point of the major weight-loss stage ( $T_a$ ; Table 3). It was also noted that the start point of the major weight-loss stage ( $DTG > 0.1$  mg/min) was delayed, while the temperature range of the major weight-loss stage ( $T_a$  to  $T_c$ ; Table 3) changed in the presence of SBA-15, La/SBA-15, and Fe/La/SBA-15, indicating that the presence of catalysts affected the major weight-loss process to varying degrees. When the temperatures were higher than about 850 °C, there was a small weight loss stage with the presence of catalysts, bringing about a reduction in the residue yield, especially for the SBA-15 catalytic test. This is probably due to some macromolecular compounds becoming coked in the pores of SBA-15 material at lower temperature. The

ordered mesoporous structure of the SBA-15 material favored the thermal cracking of the coke at high temperatures (Lu *et al.* 2009).

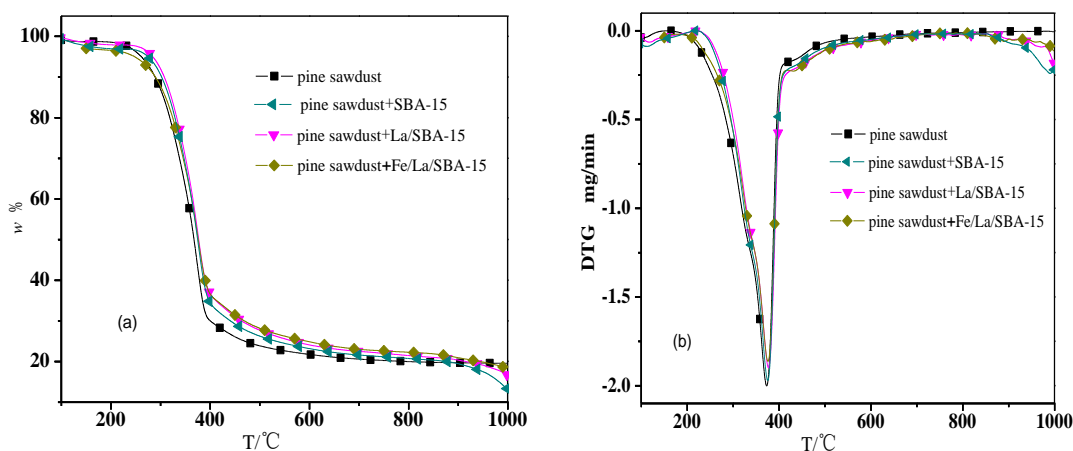


Fig. 4. The TG and DTG curves of pine sawdust pyrolysis under different catalytic conditions

Table 3. The Characteristic Points of the TG and DTG Curves for Non-catalytic and Catalytic Pyrolysis of Pine Sawdust with SBA-15 and La/SBA-15 Catalysts

Samples	$T_a$ (°C)	$T_b$ (°C)	$T_c$ (°C)	$(dw/dt)_{max}$ (mg/min)	$W_a$ (%)	$W_b$ (%)	$W_c$ (%)	$W_d$ (%)
Non-catalytic	226	373	471	-2.001	97.93	45.17	24.94	19.53
SBA-15	256	376	494	-1.974	96.41	48.87	26.56	13.35
La/SBA-15	260	376	512	-1.899	97.24	50.82	27.16	16.81
Fe/La/SBA-15	234	376	510	-1.866	95.77	49.97	27.75	18.38

a start of major weight-loss stage (DTG tends to be greater than 0.1 mg/min)

b peak point of the DTG curve

c end of major weight-loss stage (DTG tends to be smaller than 0.1 mg/min)

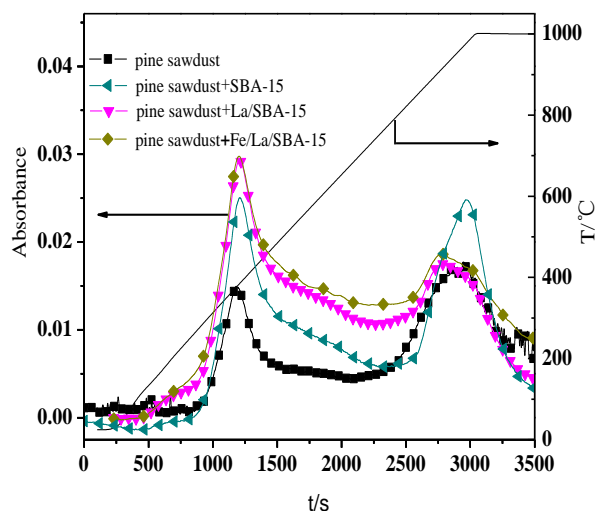
d temperature = 1000 °C

## FTIR Analyses of Gas Products

Pyrolysis vapor released from pine sawdust pyrolysis was carried into the FTIR spectrometer through a transfer tube, which is kept at about 200 °C to prevent the condensation of pyrolysis vapor on the tube wall. Evolved light gases ( $\text{CO}_2$ ,  $\text{CO}$ , and  $\text{CH}_4$ ) from the TGA were easily detected online by the FTIR spectrometer. The interest of this study was the evolution of the light gases from the pine sawdust pyrolysis, in order to lay a foundation for the subsequent biomass catalytic pyrolysis and gasification experiments in a bubbling fluidized bed reactor for gaseous fuels. The characteristic IR peaks of the light gases are  $3014\text{ cm}^{-1}$ ,  $2358\text{ cm}^{-1}$ , and  $2180\text{ cm}^{-1}$  for  $\text{CH}_4$ ,  $\text{CO}_2$ , and  $\text{CO}$ , respectively (Biagini *et al.* 2006). The evolution curves of the light gases characterized by FTIR are shown in Figs. 5 through 7.

Figure 5 shows the evolution of  $\text{CO}$  from the pyrolysis of pine sawdust under different catalytic conditions, which were monitored by FTIR. The formation of  $\text{CO}$  was mostly from the decomposition of carbonyl and carboxyl groups. These groups can be generated during pyrolysis of cellulose, through various reactions such as dehydration, ring scission. As shown in Fig. 5, the pyrolysis evolution curves of  $\text{CO}$  appeared as two peaks in the presence or absence of catalysts. The first peak of the  $\text{CO}$  evolution curves corresponded to the  $(dw/dt)_{max}$  of the DTG curves. The formation of  $\text{CO}$  at this stage

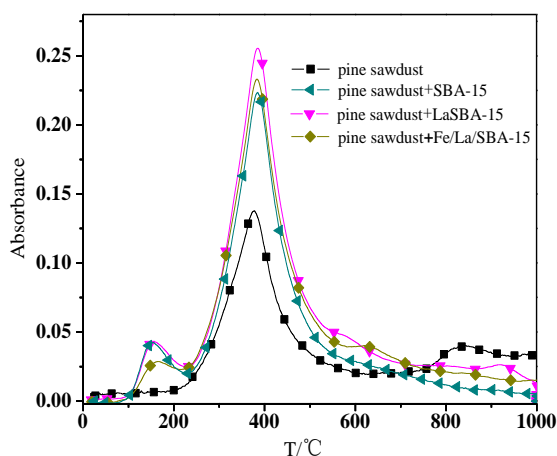
(around 376 °C) was primarily due to the decarbonylation of primary volatile products. A larger portion of the CO was released when the temperature was greater than 700 °C; this peak occurred at 968 °C without catalyst and with SBA-15, and at 916 °C with La/SBA-15 and Fe/La/SBA-15 catalysts. This was due to the polymer condensation and second thermal cracking of macromolecular polymers (Worasuwannarak *et al.* 2007). In addition, another source for the formation of CO is that the reaction between CO<sub>2</sub> and C gives 2CO, which runs at higher temperatures. This fits with the absence of any CO<sub>2</sub> production (as shown in Fig. 6) at higher temperatures simply because it reacts away. With the addition of SBA-15, the temperatures correspond to the two peaks of concentrations for CO was consistent with that in the non-catalytic test, but the released CO was significantly increased. The mesoporous structure of SBA-15 allowed large molecules into its pores, thus assisting the cracking of large molecules into smaller compounds at high temperatures (Lu *et al.* 2009). The result was an increase in the yield of CO. In the presence of modified SBA-15 materials, the temperatures of the first peak were still at 376 °C, while the second peak shifted to lower temperatures. Compared with the non-catalyzed or SBA-15 catalytic runs, the amount of CO released was increased with the modified SBA-15 catalysts, especially with Fe/La/SBA-15. This suggested that the modified SBA-15 catalysts probably catalyzed the decarbonylation reactions and the thermal cracking of some macromolecular polymers. Moreover, the second peak shifted to lower temperatures and the small peak (819 °C) in the CO<sub>2</sub> curve (in Fig. 6) disappeared in the presence of catalysts. This suggested that the catalysts may favor the reaction:  $C+CO_2 \rightarrow 2CO$ .



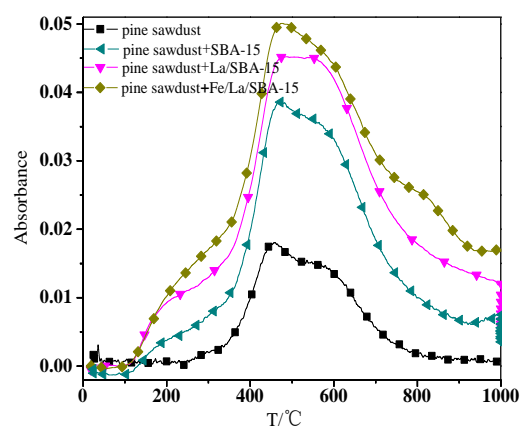
**Fig. 5.** The evolution of CO from pine sawdust pyrolysis under different catalytic conditions as monitored by FTIR

Figure 6 shows the evolution of CO<sub>2</sub> from pine sawdust pyrolysis under different catalytic conditions, as monitored by FTIR. The evolution curves of CO<sub>2</sub> appeared as only one primary peak, which was also close to the point of  $(dw/dt)_{max}$ . In the higher temperature range, the release of CO<sub>2</sub> was not obvious, which suggested that the formation mechanism of CO<sub>2</sub> was different from that of CO. CO<sub>2</sub> was formed mostly from carboxyl groups. In the presence of SBA-15, La/SBA-15, and Fe/La/SBA-15, the peak of the CO<sub>2</sub> evolution curve in all the runs shared the same temperature. From Fig. 6,

it can be noted that the absorption value was significantly enhanced in the presence of catalysts, indicating the addition of catalysts favored the decarboxylation in the major weight loss stage during the pine sawdust pyrolysis process.



**Fig. 6.** The evolution of CO<sub>2</sub> from pine sawdust pyrolysis under different catalytic conditions as monitored by FTIR



**Fig. 7.** The evolution of CH<sub>4</sub> from pine sawdust pyrolysis under different catalytic conditions as monitored by FTIR

As shown in Figure 7, the release curve of CH<sub>4</sub> reached its peak at temperatures higher than that of the  $(dw/dt)_{max}$  value of the DTG curves. More energy was required to cleave the R-CH<sub>3</sub> bonds to form CH<sub>4</sub> (Shen and Gu 2009), which was likely why the peak temperature was higher. There are many methoxyl groups in the side chains of lignin. CH<sub>4</sub> could arise from two sources during pine sawdust pyrolysis: the first peak (441 °C) in the pine sawdust run was primarily due to the decomposition of methoxyl groups, while the shoulder peak (about 590 °C) was attributed to decomposition of the hydrocarbon skeleton after deoxygenation at higher temperatures (Biagini *et al.* 2006; Sun *et al.* 2011). When comparing the evolution of CH<sub>4</sub> during pine sawdust pyrolysis in the presence of different catalysts, it can be concluded that the modified SBA-15 materials favored the catalytic cracking and reforming of carbon skeleton, and then the CH<sub>4</sub> yield was improved significantly. Moreover, reactions (Eqs. 1 and 2) may be accelerated due to the catalysts. Methane has a high heating value, and the attempt of increasing its content in the gaseous product of biomass pyrolysis may benefit for producing a gaseous fuel with higher heating value.



Figures 5 through 7 display the evolution curves of CO, CO<sub>2</sub>, and CH<sub>4</sub>, respectively. According to these figures, it can be seen that the peak value increase from 0.015 to 0.03 for CO, from 0.14 to 0.26 for CO<sub>2</sub>, and from 0.018 to 0.049 for CH<sub>4</sub>. Hence there is an increase in the selectivity of CH<sub>4</sub>, and a slight increase for CO selectivity, giving a producer gas with higher heating value in the presence of the Fe/La/SBA-15 material.

## CONCLUSIONS

1. Modified SBA-15 catalysts were well prepared in this study. The La/SBA-15 catalyst was synthesized through an *in-situ* hydrothermal method, and then the Fe/La/SBA-15 catalyst was prepared by the impregnation of iron into the existing La/SBA-15 material. These catalysts retained the hexagonal order of the SBA-15 support material and showed high thermal stability in the temperature range examined.
2. The effects of the modified SBA-15 catalysts on the formation characteristics of pine sawdust pyrolysis vapor were studied by TG-FTIR. The analysis showed that the pyrolysis behavior of the biomass was remarkably improved in the presence of La/SBA-15 and Fe/La/SBA-15 catalysts. The gas yield was significantly increased, especially in terms of the increased yield of CH<sub>4</sub>. And there was a reduction in the yields of tar and char. Therefore, it can be concluded that the modified SBA-15 catalysts favored the cracking or reforming of tar content during the pyrolysis process, especially in the presence of Fe/La/SBA-15.

## ACKNOWLEDGMENTS

The authors greatly acknowledge funding from projects supported by the National Basic Research Program of China (973 Program; Grant No. 2010CB732206), the National Natural Science Foundation of China (Grant No. 51306036), and the Major Research Plan of National Natural Science Foundation of China (Grant No. 91334205). Additionally, the authors are grateful for the kind support from the Committee of the 4<sup>th</sup> Conference on Biorefinery towards Bioenergy (ICBB 2013) in Xiamen, China.

## REFERENCES CITED

- Abu El-Rub, Z., Bramer, E., and Brem, G. (2004). "Review of catalysts for tar elimination in biomass gasification processes," *Ind. Eng. Chem. Res.* 43(22), 6911-6919.
- Bendahou, K., Cherif, L., Siffert, S., Tidahy, H., Benaissa, H., and Aboukais, A. (2008). "The effect of the use of lanthanum-doped mesoporous SBA-15 on the performance of Pt/SBA-15 and Pd/SBA-15 catalysts for total oxidation of toluene," *Applied Catalysis A: General* 351(1), 82-87.
- Biagini, E., Barontini, F., and Tognotti, L. (2006). "Devolatilization of biomass fuels and biomass components studied by TG/FTIR technique," *Ind. Eng. Chem. Res.* 45(13), 4486-4493.
- Carlson, T. R., Vispute, T. P., and Huber, G. W. (2008). "Green gasoline by catalytic fast pyrolysis of solid biomass derived compounds," *ChemSusChem.* 1(5), 397-400.
- Chen, G. and Leung, D. (2003). "Experimental investigation of biomass waste, (rice straw, cotton stalk, and pine sawdust), pyrolysis characteristics," *Energy Sources.* 25(4), 331-337.
- Chen, Y., Huang, Y., Xiu, J., Han, X. and Bao, X. (2004). "Direct synthesis, characterization and catalytic activity of titanium-substituted SBA-15 mesoporous molecular sieves," *Applied Catalysis A: General.* 273(1), 185-191.

- Dayton, D. (2002). "A review of the literature on catalytic biomass tar destruction," NREL Report, NREL/TP-510-32815, NREL, Golden, CO.
- Devi, L., Ptasiński, K. J., and Janssen, F. J. (2003). "A review of the primary measures for tar elimination in biomass gasification processes," *Biomass Bioenerg.* 24(2), 125-140.
- Groen, J. C., Peffer, L. A., and Pérez-Ramírez, J. (2003). "Pore size determination in modified micro- and mesoporous materials. Pitfalls and limitations in gas adsorption data analysis," *Micropor. Mesopor. Mat.* 60(1), 1-17.
- Koufopoulos, C., Lucchesi, A., and Maschio, G. (1989). "Kinetic modelling of the pyrolysis of biomass and biomass components," *The Canadian Journal of Chemical Engineering* 67(1), 75-84.
- Lansink Rotgerink, H. G. J., Paalman, R. P. A. M., van Ommen, J. G., and Ross, J. R. H. (1988). "Studies on the promotion of nickel—alumina coprecipitated catalysts: II. Lanthanum oxide," *Applied catalysis.* 45(2), 257-280.
- Lu, Q., Li, W., Zhang, D., and Zhu, X. (2009). "In situ catalytic cracking of sawdust fast pyrolysis vapors," *Journal of Chemical Industry and Engineering (China)*. 60(2): 351-357.
- Martinez, R., Romero, E., Garcia, L. and Bilbao, R. (2004). "The effect of lanthanum on Ni–Al catalyst for catalytic steam gasification of pine sawdust," *Fuel Process. Technol.* 85(2), 201-214.
- Nguyen, T., Zavarin, E., and Barrall, E. M. (1981). "Thermal Analysis of lignocellulosic materials: Part I. Unmodified materials," *J. Macromol. Sci.-Rev. Macromol. Chem., C.* 20(1), 1-65.
- Nguyen, T., Zabeti, M., Lefferts, L., Brem, G., and Seshan, K. (2013). "Catalytic upgrading of biomass pyrolysis vapours using faujasite zeolite catalysts," *Biomass Bioenerg.* 48,100-110.
- Nordgreen, T., Liliedahl, T., and Sjöström, K. (2006). "Elemental iron as a tar breakdown catalyst in conjunction with atmospheric fluidized bed gasification of biomass: A thermodynamic study," *Energy. Fuels.* 20(3), 890-895.
- Raveendran, K., and Ganesh, A. (1996). "Heating value of biomass and biomass pyrolysis products," *Fuel.* 75(15), 1715-1720.
- Ren, S., Lei, H., Wang, L., Bu, Q., Chen, S., Wu, J., Julson, J. and Ruan, R. (2013). "The effects of torrefaction on compositions of bio-oil and syngas from biomass pyrolysis by microwave heating," *Bioresour. Technol.* 135: 659-664.
- Richardson, S. M. and Gray, M. R. (1997). "Enhancement of residue hydroprocessing catalysts by doping with alkali metals," *Energy. Fuels.* 11(6), 1119-1126.
- Scott, D. S., Piskorz, J. and Radlein, D. (1985). "Liquid products from the continuous flash pyrolysis of biomass," *Ind. Eng. Chem. Proc. D. D.* 24(3), 581-588.
- Shen, D., and Gu, S. (2009). "The mechanism for thermal decomposition of cellulose and its main products," *Bioresour. Technol.* 100(24), 6496-6504.
- Sing, K. S. W., Everett, D. H., Haul, R. A. W., Moscou, L., Periotti, R. A., Rouquérol, J., and Siemieniewska, T. (1985). "Reporting physisorption data for gas/solid systems with special reference to the determination of surface area and porosity," *Pure Appl. Chem.* 57(4), 603-619.
- Sun, M., Ma, X.-X., Yao, Q.-X., Wang, R.-C., Ma, Y.-X., Feng, G., Shang, J.-X., Xu, L. and Yang, Y.-H. (2011). "GC-MS and TG-FTIR study of petroleum ether extract and residue from low temperature coal tar," *Energy. Fuels.* 25(3), 1140-1145.

- Sun, Y., Walspurger, S., Tessonnier, J.-P., Louis, B., and Sommer, J. (2006). "Highly dispersed iron oxide nanoclusters supported on ordered mesoporous SBA-15: A very active catalyst for Friedel–Crafts alkylations," *Applied Catalysis A: General*. 300(1), 1-7.
- Tamhankar, S. S., Tsuchiya, K. and Riggs, J. B. (1985). "Catalytic cracking of benzene on iron oxide-silica: Catalyst activity and reaction mechanism," *Applied Catalysis* 16(1), 103-121.
- Wang, D., Xiao, R., Zhang, H., and He, G. (2010). "Comparison of catalytic pyrolysis of biomass with MCM-41 and CaO catalysts by using TGA–FTIR analysis," *J. Anal. Appl. Pyrolysis*. 89(2), 171-177.
- Worasuwannarak, N., Sonobe, T., and Tanthapanichakoon, W. (2007). "Pyrolysis behaviors of rice straw, rice husk, and corncob by TG-MS technique," *J. Anal. Appl. Pyrolysis*. 78(2), 265-271.
- Yang, H., Yan, R., Chen, H., Lee, D. H., and Zheng, C. (2007). "Characteristics of hemicellulose, cellulose and lignin pyrolysis," *Fuel*. 86(12), 1781-1788.
- Zhang, H., Xiao, R., Jin, B., Shen, D., Chen, R., and Xiao, G. (2013a). "Catalytic fast pyrolysis of straw biomass in an internally interconnected fluidized bed to produce aromatics and olefins: Effect of different catalysts," *Bioresour. Technol.* 137,82-87.
- Zhang, H., Zheng, J., Xiao, R., Shen, D., Jin, B., Xiao, G., and Chen, R. (2013b). "Co-catalytic pyrolysis of biomass and waste triglyceride seed oil in a novel fluidized bed reactor to produce olefins and aromatics integrated with self-heating and catalyst regeneration processes," *RSC Advances* 3(17), 5769-5774.
- Zhao, D., Feng, J., Huo, Q., Melosh, N., Fredrickson, G. H., Chmelka, B. F. and Stucky, G. D. (1998). "Triblock copolymer syntheses of mesoporous silica with periodic 50 to 300 angstrom pores," *Science* 279(5350), 548-552.

Article submitted: January 14, 2014; Peer review completed: May 8, 2014; Revised version received: July 2, 2014; Accepted: July 3, 2014; Published: July 16, 2014.